Chapter 53
Synthesis and Characterization of Novel Oxides as Active Material in Lithium Ion Batteries

D. Nicheva, T. Stankulov, D. Blyskova-Koshnicharova, E. Lefterova, O. Koleva, A. Momchilov, and T. Petkova

Abstract The aim of the present work is the synthesis and characterization of novel oxide materials in view of their potential use as active material in lithium ion batteries. Bulk materials from $(TiO_2)_x(V_2O_5)_y(P_2O_5)_{100-x-y}$ system, where $x = 5$, 10, 15 and $y = 60$, 70, were prepared by means of the melt quenching method. The materials were characterized by physical chemical and electrochemical methods, i.e. X-ray diffraction, infrared spectroscopy and cyclic voltammetry measurements. The electrochemical properties were investigated against metallic lithium as active materials in a half-cell system.

Keywords Phosphate glasses • Lithium ion batteries

53.1 Introduction

The limited amount of fossil fuels and growing environmental problem associated with their production and combustion leads to an continuously increasing need for renewable energy sources and storage methods. Lithium batteries (LIBs) are the systems of choice, offering high energy densities, flexible, lightweight design and longer lifespan than comparable battery technologies [1]. Besides high-power high-energy-density applications and, in addition vehicular transport, LIBs are also actively being considered for power tools, back-up power supply units, and off-peak energy storage (load leveling) from the electric grid for civil, but also for military supplies. For all these uses, LIBs need to satisfy four important criteria [2]:

D. Nicheva (✉) • T. Stankulov • D. Blyskova-Koshnicharova • E. Lefterova • O. Koleva
A. Momchilov • T. Petkova
Institute of Electrochemistry and Energy Systems Acad. E. Budevski,
Bulgarian Academy of Sciences, Bl.10 Acad. G. Bonchev Str., 1113 Sofia, Bulgaria
e-mail: denitza_vladimirova@abv.bg

P. Petkov et al. (eds.), *Nanoscience Advances in CBRN Agents Detection, Information and Energy Security*, NATO Science for Peace and Security Series A: Chemistry and Biology, DOI 10.1007/978-94-017-9697-2_53

(1) cost reduction, (2) improvement of the energy density from ~120 to ~250 Wh/kg, (3) safety-in-operation and (4) improvements of low- as well as high-temperature operation.

One way to achieve higher capacities is to use an electrode material in which the metal ion can change its oxidation state by two or more units. In this study we present the results of our investigation of the TiO_2-V_2O_5-P_2O_5 system in view of electrochemical application.

53.2 Experimental Details

Bulk materials from the $(TiO_2)_x(V_2O_5)_y(P_2O_5)_{100-x-y}$ system, where $x = 5, 10, 15$ % and $y = 60, 70$ %, were prepared by means of the melt quenching method from TiO_2 and V_2O_5 powders and liquid orthophosphoric acid H_3PO_4 as precursors. The initial materials were mixed for better homogenization, placed in a quartz crucible and melted in a high temperature furnace in air. The synthesis was carried out as follows: the temperature was increased stepwise to 1,200 °C, the melt was kept for 1.5 h at 1,200 °C and quenched between copper plates.

XRD analyses were performed by using a X-ray diffractometer model Philips APD-15. The data were collected at ambient temperature with a constant step of 0.02 deg·s^{-1} from angles $2\theta = 20 - 60°$ at the wavelength $\lambda = 1.54178$ Å using a CuKα tube. The structure of the materials was studied by means of an FTIR spectrometer model VARIAN 660-IR.

The electrodes were prepared by spreading them (one-side) on an Al foil. Electrodes consisting of 50 % (w/o) active materials and 50 wt% conductive binder (TAB2, teflonized acetylene black) were dried at 120 °C in a vacuum oven for 12 h and then pressed to enhance the contact between the active materials and the conductive carbons. Galvanostatic tests were carried out in a three-electrode half cell (the prototype of the 2032 button cell), using a metallic Li foil as both counter and reference electrode. The electrolyte used was 1 M $LiPF_6$ dissolved in a mixture of ethylene carbonate (EC) and dimethyl carbonate (DMC) (1:1 in vol.). The cells were assembled in a glove box under highly pure dry argon atmosphere. Cyclic voltammograms (CVs) were measured with an Autolab PSTAT 10 with a scan rate of 0.05 mV/s in the potential range from 1.5 to 3.5 V. Constant current (CC) tests were performed with the aid of an Arbin Instruments BT 2000. The capacities C of materials were based on the experimentally obtained data from the CV tests of the materials.

53.3 Results and Discussion

53.3.1 X-ray Diffraction Analysis

The XRD analyses used to prove the nature of the samples show that $(TiO_2)_5(V_2O_5)_{70}(P_2O_5)_{25}$ and $(TiO_2)_{15}(V_2O_5)_{70}(P_2O_5)_{15}$ compounds are amorphous (Fig. 53.1a). The diffractogram of $(TiO_2)_{10}(V_2O_5)_{60}(P_2O_5)_{30}$ (Fig. 53.1b) displays

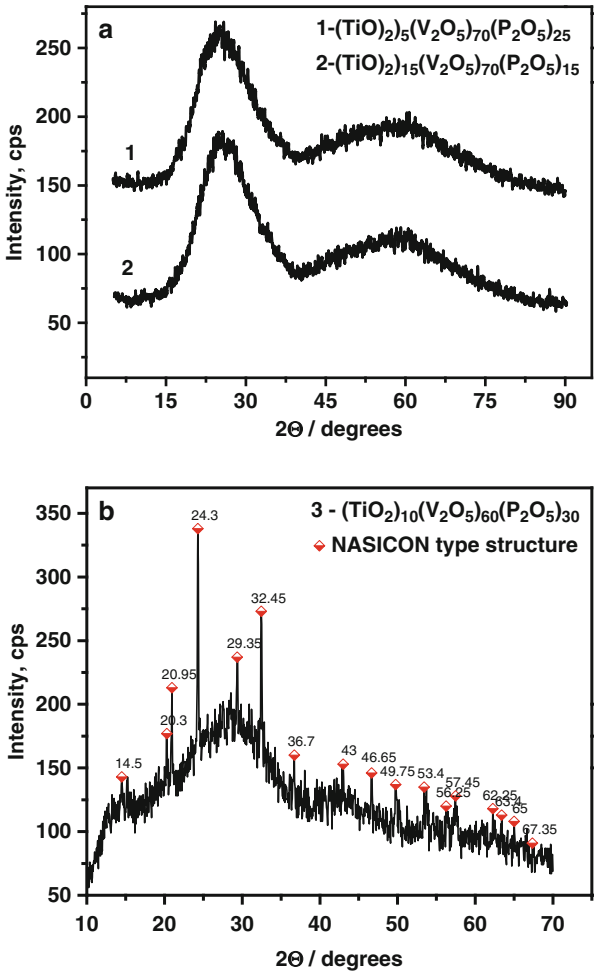

Fig. 53.1 XRD diffractograms of (**a**): $(TiO_2)_5(V_2O_5)_{70}(P_2O_5)_{25}$ (*1*), $(TiO_2)_{15}(V_2O_5)_{70}(P_2O_5)_{15}$ (*2*) and (**b**): $(TiO_2)_{10}(V_2O_5)_{60}(P_2O_5)_{30}$ (*3*)

amorphous an halo and weak peaks indicating crystalline phases distributed in the amorphous oxide matrix. The peaks positions are very similar to those of $Ti_4P_6O_{23}$, $NaTi_2(PO_4)_3$ and $NaVTi(PO_4)_3$. These peaks validate the presence a NASICON type structure (Na super ionic conductor) in the samples of this study [3, 4].

53.3.2 Infrared Study

Infrared spectra of $(TiO_2)_x(V_2O_5)_y(P_2O_5)_{100-x-y}$ glassy system are presented in Fig. 53.2. The band at 1,005 cm^{-1} can be attributed both to VO_5-groups and to isolated PO_4^{3-} (Q^0) phosphate groups observed for $(TiO_2)_5(V_2O_5)_{70}(P_2O_5)_{25}$ and $(TiO_2)_{15}(V_2O_5)_{70}(P_2O_5)_{15}$ glasses. The band splits into two peaks located

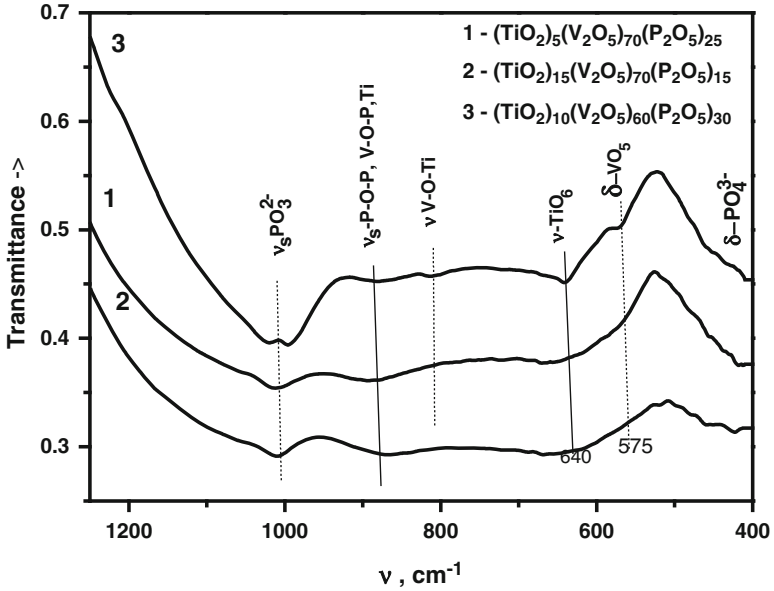

Fig. 53.2 Infrared spectra of $(TiO_2)_x(V_2O_5)_y(P_2O_5)_{100-x-y}$ glassy sample

at 990 and 1,020 cm^{-1} with increasing TiO_2 and P_2O_5 content probably due to the appearance of VO_4 groups that occupy octahedral positions in the NASICON structure.

The wide absorption band between 600 and 670 cm^{-1} originates from TiO_6 octahedra, while absorption below 600 cm^{-1} is due to bending vibrations of VO_5-groups and to the network vibrations.

Three other bands located at 640, 575 and 811 cm^{-1} are indicated. We can very likely assign the 640 cm^{-1} band to TiO_6 groups as part of the NASICON structure, the 811 cm^{-1} mode might be attributed to mixed V-O-Ti bonds.

The structure of phosphate glasses might be considered as a polymeric network composed of tetrahedral $[PO_4]$ groups. The structure is usually determined by Q^n molecules, where n stands for the number of bridged oxygen atoms in a tetrahedron. Depending on the [O]/[P] ratio phosphor-containing amorphous materials can be composed of: (a) a network of Q^3 tetrahedra (in glassy P_2O_5) with asymmetric stretching vibrations of the P=O bond at ~1,270 cm^{-1}, (b) polymeric metaphosphate chains of Q^2 tetrahedra $(PO_2)^-$ with asymmetric bond vibrations at ~1,280 cm^{-1} and symmetric stretching vibrations at 1,100 cm^{-1}, (c) "inverted" glasses, based on Q^1 with a structural unit of $(PO_3)^{2-}$ groups with stretching vibrations at ~1,050 cm^{-1}, and (d) orthophosphate Q^0 with the main structural group of $(PO_4)^{3-}$ tetrahedra the stretching of which is located at 1,000 cm^{-1}. Addition of TiO_2 to the phosphate glasses enhances the glass forming ability, chemical stability and compactness of the structure. TiO_2 as glass modifyer contributes to the appearance of non-bridged oxygen atoms in the glass and

depolymerization of the phosphate network after distortion of the P-O-P bridge structure. The IR spectra of glassy and crystalline V_2O_5 are comparable with difference in the peak sharpness. They consist of deformed trigonal bi-pyramids of VO_5 groups with one vanadium ion in the center of the polyhedron and one shorter V=O (vanadyl) bond.

The results of the IR study show that the material is composed of TiO_6 octahedron connected to six PO_4 tetrahedra building a NASICON structure. They form 3D interconnected channels with two types of empty positions occupied to some extent by VO_5 groups. The existence of VO_5 groups and isolated PO_4^{3-} (Q^0) structural units, as well as TiO_6-octahedra was proven for all materials. When the TiO_2 and P_2O_5 content increases, new structural unit of VO_4 groups are formed.

53.3.3 Electrochemical Investigations

The CV-curves of the electrodes under study are presented in Fig. 53.3. The peak appearing at potentials of about 2.5 V in the CV curve can be assigned to some structural reorganisation in the compounds. The effect has been ascribed to different factors, including structural effects after reduction of V^{5+} to V^{4+} and lithium incorporation into the structure (electrochemical lithiation). We assume that probably lithium ions occupy the empty positions in the NASICON structure or/and form new bonds.

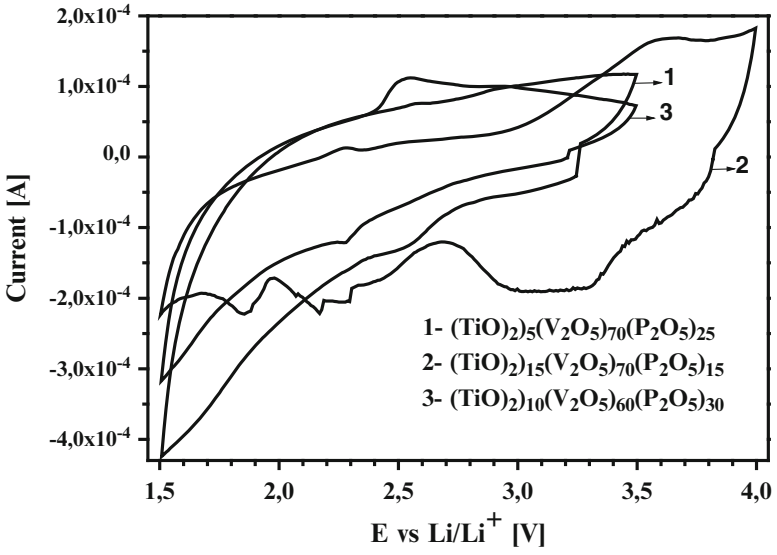

Fig. 53.3 Cyclic voltammogram curves of the materials with a scan rate of 0.05 mV/s

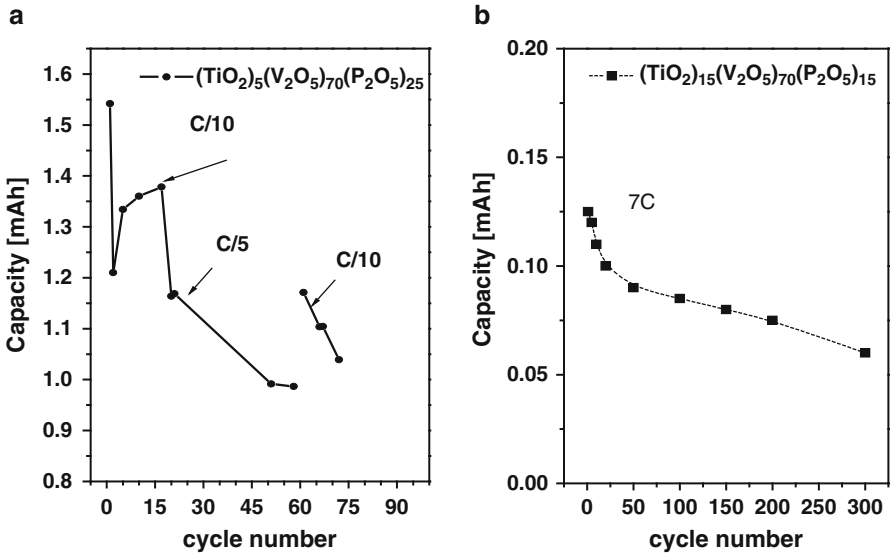

Fig. 53.4 Discharge capacity vs. cycle number of (**a**) $(TiO_2)_5(V_2O_5)_{70}(P_2O_5)_{25}$ and (**b**) $(TiO_2)_{15}(V_2O_5)_{70}(P_2O_5)_{15}$ for various C-rates

The electrochemical lithiation of $(TiO_2)_5(V_2O_5)_{70}(P_2O_5)_{25}$ shows 38 % increase during the first CV cycle; the increase is higher after the second (79 %) and the third cycle (93 %).

The discharge capacity of the $(TiO_2)_5(V_2O_5)_{70}(P_2O_5)_{25}$ was tested at various current rates (Fig. 53.4a). The material shows a stable capacity after 15 cycles with a C/10-rate (the C-rate is a standard charge-discharge regime for electrochemical power sources, where the current is expressed by means of the electrode capacity). The capacity increases by 23 %, analogous to that observed in the CV test, and decreases by 16 % during the further study with a current of C/5 rate.

The CV results of the $(TiO_2)_{15}(V_2O_5)_{70}(P_2O_5)_{15}$ compound (Fig. 53.3) shows electrochemical activity of the material above 4.0 V. To this end CC cycling tests were carried out with a high current of 7C (Fig. 53.4b). The results reveal a capacity of 12.5 % obtained from CV test. The material lost 28 % of the capacity after 50 cycles, 11 % during the next 100–200 cycles, and 20 % during the cycles 200–300.

53.4 Conclusions

Bulk materials from $(TiO_2)_x(V_2O_5)_y(P_2O_5)_{100-x-y}$ system, where $x = 5$, 10, 15 and $y = 60$, 70 were synthesized and characterized. It was found that $(TiO_2)_5(V_2O_5)_{70}(P_2O_5)_{25}$ and $(TiO_2)_{15}(V_2O_5)_{70}(P_2O_5)_{15}$ are amorphous, while $(TiO_2)_{10}(V_2O_5)_{60}(P_2O_5)_{30}$ consists of an amorphous matrix with nanocrystals of the NASICON type. IR investigation showed the presence of VO_5 groups and

isolated PO_4^{3-} (Q^0) structural units, as well as TiO_6-octahedra in all materials. When the TiO_2 and P_2O_5 content increases, new structural units of VO_4 groups are formed. The electrochemical properties were investigated against metallic lithium as active materials in a half-cell system. The results show that the studied oxides possess rechargeable Li intercalation due to the presence of V_2O_5. The $(TiO_2)_{15}(V_2O_5)_{70}(P_2O_5)_{15}$ compound has an electrochemical activity at 4 V, i.e. the material is suitable for application as active element in high voltage lithium-ion batteries.

References

1. Van Schalkwijk W, Scrosati B (eds) (2002) Advances in lithium-ion batteries. Springer, Berlin
2. Reddy MV, Subba Rao GV, Chowdari BV (2013) Chem Rev 113:5364
3. Agaskar PA, Grasselli RK, Butterey DJ, White B (1997) In: Oyama ST, Gaffney AM, Lyons JE, Grasselli RK (eds) Third World Congress on Oxidation Catalysis. Elsevier, Amsterdam, p 219
4. Dimitrov V, Dimitriev Y (2009) Structural analysis. UCTM, Sofia